DOI 10.5012/bkcs.2010.31.11.3241

Biochemical and Biophysical Characterizations of the Interaction between Two PDZ Adapter Proteins NHERF and E3KARP *in vitro*

Eun Young Hwang,[a] Mi Suk Jeong,[a] and Se Bok Jang[*]

Department of Molecular Biology, College of Natural Sciences, Pusan National University, Busan 609-735, Korea
[*]E-mail: sbjang@pusan.ac.kr
Received August 10, 2010, Accepted September 14, 2010

NHERF (Na^+/H^+ exchanger regulatory factor) and E3KARP (NHE3 kinase A regulatory protein) play important roles in membrane targeting, trafficking and sorting of ion channels, transmembrane receptors and signaling proteins in many tissues. Each of these proteins contains two PDZ (PSD-95/Dlg-1/ZO-1) domains, which mediate the assembly of transmembrane and cytosolic proteins into functional signal transduction complexes. The interaction between NHERF and E3KARP was investigated by surface plasmon resonance spectroscopy (BIAcore), fluorescence measurement, His-tagged pull-down experiment, and size-exclusion column (SEC) chromatography. BIAcore experiments revealed that NHERF bound to E3KARP with an apparent K_D of 7 nM. Fluorescence emission spectra of the NHERF-E3KARP complex suggested that the tight interaction between these proteins was accompanied by significant conformational changes in one or both. The CD spectra of NHERF and E3KARP show that the conformational changes of these proteins were dependent on pH and temperature. These results implicate that the NHERF-E3KARP complex allows intracellular signaling complexes to form through PDZ-PDZ interactions.

Key Words: NHERF, E3KARP, Interaction, Biochemical characterization

Introduction

PDZ (PSD-95/Dlg-1/ZO-1) proteins participate in scaffolding multiprotein complexes, targeting, and regulation of membrane proteins.[1,2] They amplify their capacity and diversity of protein-protein interactions through co-expression of protein-binding motifs (e.g. SH2 domains, SH3 domains, ankyrin repeats, ERM binding domains), expression of multiple PDZ domains within the same PDZ protein, and oligomerization with other PDZ proteins.[3,4] The PDZ-fold comprises a six-stranded antiparallel β-barrel capped by two α-helices.[5-10]

NHERF and E3KARP, two tandem PDZ domain-containing proteins, were originally identified as regulatory proteins of the protein kinase A (PKA)-dependent regulation of NHE3.[11,12] Both NHERF and E3KARP interact with NHE3 through their C-terminally extended second PDZ domain (P2C). In addition, the last 30 amino acids of these PDZ domain proteins interact with ezrin. Ezrin is thought to act as a kinase-anchoring protein, which physically locates PKA in close proximity to NHE3.[13] These PDZ domain proteins are necessary for cAMP-induced inhibition of NHE3 activity by allowing PKA-dependent phosphorylation of NHE3.[14] Additionally, NHERF and E3KARP are structurally-related protein adapters that are highly expressed in epithelial tissues. Since they are closely related in structure and sequence and appear to belong to the same family of proteins, E3KARP is sometimes referred to as NHERF2. Human NHERF is a 358-residue protein containing two PDZ domains (residues 11-97 and 150-237) followed by ~120 C-terminal residues.[15] E3KARP consists of 337 residues along with two PDZ and EB (ERM binding) domains.

The NHERF PDZ1 domain interacts with the motifs DSLL, DSFL and DTRL present at the carboxyl termini of β_2 adrenergic receptor (β_2AR), platelet-derived growth factor receptor (PDGFR) and cystic fibrosis transmembrane conductance regulator (CFTR), respectively.[16,17] The highly homologous PDZ proteins NHERF and E3KARP may function similarly in the membrane trafficking/anchoring and regulation of both CFTR and NHE3.[18] The regulation of CFTR activity, as well as that of intestinal salt absorptive transporter NHE3, occurs *via* the formation of PDZ adapter protein-mediated multiprotein complexes.

To determine whether or not NHERF and E3KARP interact as members of the same trafficking pathway, recombinant NHERF and E3KARP were isolated and purified. We show through a series of biochemical and biophysical measurements that NHERF interacted with E3KARP *in vitro*. These studies provide important clues to the structural identification of membrane signaling pathways involving NHERF and E3KARP.

Materials and Methods

Cloning, expression, and purification. Full-length NHERF (1-358 aa) and E3KARP (1-337 aa) were subcloned into N-terminal His-tagged fusion protein vector pET-30a. The positive His_6-NHERF and E3KARP expression plasmids were identified by restriction endonuclease digestion and further verified by DNA sequencing using a Macrogen automatic DNA sequencer. The constructs were transformed into the expression host *Escherichia coli* BL21(DE3), followed by expression and purification as previously described.[19] Isolated NHERF and E3KARP had observed molecular weights of approximately 57 kDa and 47 kDa, respectively. We obtained soluble proteins at final concentrations of 12 mg/mL for NHERF and 11 mg/mL for E3KARP using a quantification kit with bovine serum.

His-tagged pull-down assay. For the pull-down experiment, His-tagged fusion protein-immobilized sepharose beads were

[a]These authors contributed equally to this article

prepared. A total of 50 μg each of purified NHERF and His-tagged E3KARP was mixed with 50 μL of Ni-metal chelating affinity resin in binding buffer (50 mM Tris-HCl, pH 7.5, 200 mM NaCl, 1 mM DTT and 0.1 mM PMSF) by rotating at 4 °C for 3 h. The supernatant was removed by centrifugation at 8000 rpm for 3 min. The beads were then washed three times with wash buffer (50 mM Tris-HCl, pH 7.5, 200 mM NaCl, 1 mM DTT and 0.1 mM PMSF). Each time, the beads were incubated with wash buffer on a rotator for 3 min and collected by centrifugation. The beads were eluted with elution buffer (50 mM Tris-HCl, pH 7.5, 200 mM NaCl, 1 mM DTT, 0.1 mM PMSF and 200 mM imidazole), boiled in SDS sample loading buffer for 5 min and then resolved by SDS-PAGE for Coomassie blue staining.

Circular dichroism (CD) and temperature controller measurements. Circular dichroism (CD) measurements were taken using a spectropolarimeter (JASCO J-815) in a 0.1 cm cell at 0.2 nm intervals at 25 °C. The CD spectra of the purified NHERF and E3KARP proteins were recorded in the range of 190 - 260 nm. Each spectrum was the average of 10 scans. Far-UV CD spectra were taken using a protein concentration of 0.5 mg/mL. The CD spectra were obtained in milli-degrees and converted to molar ellipticity prior to secondary structure analysis using the CDNN program.[20] The CD spectra of the proteins were obtained at various pH levels and adjusted with buffers. Temperature controller spectra were taken using the same set-up by heating the proteins with a constant temperature gradient from 20 °C to 60 °C.

BIAcore biosensor analysis. Measurements of the apparent dissociation constants (K_D) between NHERF and E3KARP were carried out using a BIAcore 2000 biosensor (Biosensor, Sweden). E3KARP (500 μg/mL in 10 mM sodium acetate [pH 4.0]) was covalently bound to the carboxylated dextran matrix at a concentration corresponding to ~1,200 response units (RU) by amine-coupling method, as suggested by the manufacturer. A flow path involving two cells was employed to simultaneously measure the kinetic parameters from one flow cell containing the E3KARP-immobilized sensor chip to the other flow cell containing an underivatized chip. For kinetic measurements at room temperature, NHERF samples ranging in concentration from 20 to 319 nM were prepared by dilution in HBS buffer (150 mM NaCl, 3 mM EDTA, 0.005% surfactant P20 and 10 mM HEPES [pH 7.4]). Each sample was injected with 50 μL of NHERF solution into the flow cells (association phase) at a rate of 10 μL/min. Among the cycles, the immobilized ligand was regenerated by injection with 30 μL of 50 mM NaOH at a rate 10 μL/min.

Fluorescence spectroscopy. Fluorescence emission spectra were obtained using an Edinburgh (UK) FLS920 TCSPC (Time Correlated Single Photon Counting Spectrometer) along with 1 cm path length cuvettes containing excitation and emission slits 20 nm in width. The fluorescence emission spectra of NHERF and E3KARP were obtained in order to identify characteristic chemical structures, namely double bonds and aromatic groups. The emission intensity was recorded from 305 to 465 nm at an excitation wavelength of 295 nm. NHERF and E3KARP were preincubated together for 25 min at 25 °C. The concentration of each protein was 5 μM. All spectra were obtained at a protein concentration of 50 μg/ml at 24 °C. Ten spectra of each protein sample were accumulated, averaged and subjected to baseline correction by subtracting the buffer spectrum.

Results and Discussion

NHERF and E3KARP proteins have three distinct domains (PDZ1, PDZ2 and EB domains), of which the PDZ domains are approximately equal in size (Fig. 1A). The amino acid sequences of NHERF and E3KARP are compared in Figure 1B. NHERF and E3KARP share similar domain organization, with conserved residues colored in blue. The PDZ1 (residues 9 to 97) and PDZ2 (residues 149 to 237) domains of the NHERF and E3KARP proteins are highly conserved, whereas the EB-region is less conserved. NHERF and E3KARP are structurally-related protein adapters that display 55% sequence identity. Despite the similarity between their PDZ domains, NHERF proteins present various affinities for PDZ-binding partners.[21]

The secondary structures of NHERF and E3KARP were predicted and shown in Figure 1B. The secondary structures of the PZD1 and PDZ2 domains in NHERF and E3KARP possess one alpha-helix and four beta-strands, respectively. In the structures of NHERF and E3KARP, there are short loop regions between the PDZ1 and PDZ2 domains, as well as long loop regions between the PDZ2 and EB domains. Long loop regions are often flexible and can adopt several different conformations. Such loops are frequently involved in the function of the protein and can switch from an open conformation, which allows access to the active site, to a closed conformation, which shields reactive groups in the active site.

We showed that NHERF interacted strongly with E3KARP

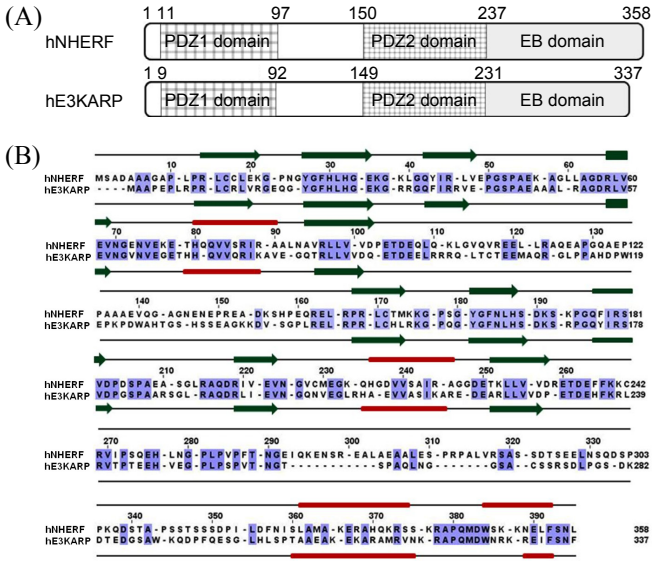

Figure 1. Domain structures, sequence alignment and predicted secondary structures of NHERF and E3KARP. A) Schematic diagram showing the domains of NHERF and E3KARP. B) Sequence alignment of the core regions of human NHERF and E3KARP. The residues that are identically conserved in the two species are in blue. The secondary structure of NHERF and E3KARP were predicted. Alpha-helices are shown as ellipses, and beta-sheets are shown as arrows. Loops are shown by gray lines. The sequences were aligned using Jalview.

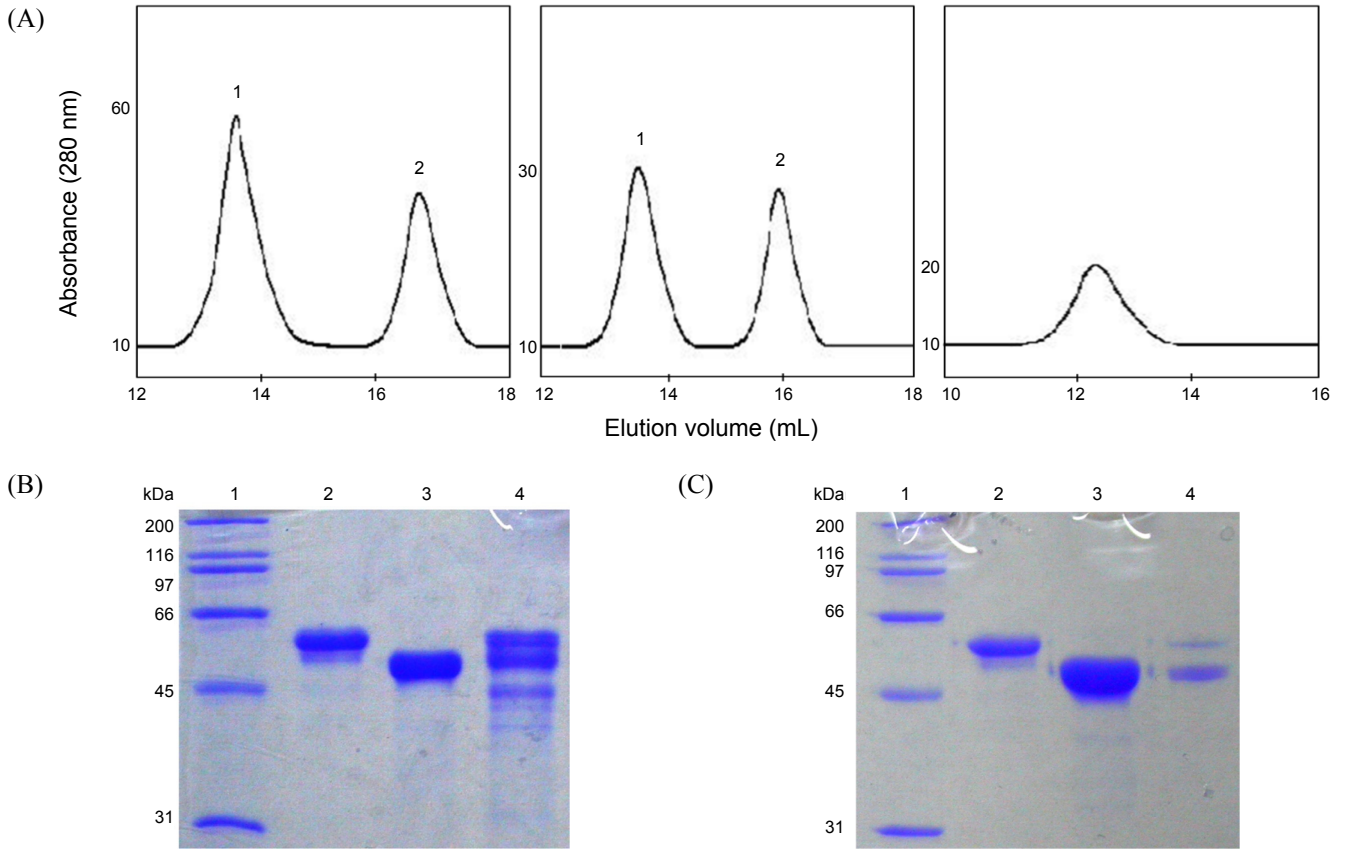

Figure 2. (A) Showing the separated fractions of proteins. Peak 1, purified NHERF (left panel); peak 1, purified E3KARP (middle panel); and NHERF-E3KARP complex eluted using a HiLoad Superdex 200 column (right panel). (B) Binding of NHERF and E3KARP is shown by SDS-PAGE analysis from size-exclusion chromatography. Lane 1: molecular marker; lane 2: NHERF; lane 3: E3KARP; lane 4: NHERF-E3KARP complex. (C) Results of His-tagged pull-down assay using His-E3KARP and NHERF *in vitro*. Lane 1: molecular marker; lane 2: NHERF; lane 3: E3KARP; lane 4: NHERF-E3KARP complex.

in vitro by a series of biochemical and biophysical measurements. The separated fractions of NHERF and E3KARP were shown in two peaks (Fig. 2A). While the band intensity was identified in the first peak, there were no bands in other peaks. The purified NHERF and E3KARP proteins were mixed in a 1:1 molar ratio. After incubation for 12 hrs at 4 °C, the mixture was loaded onto a Superdex 200 HR 10/30 size-exclusion column (SEC) (Amersham Pharmacia Biotech). Binding between NHERF and E3KARP was detected by SDS-PAGE (Fig. 2A and 2B). Further, we confirmed the interaction between NHERF and E3KARP by His-tagged pull-down assay (Fig. 2C).

To further investigate the interaction between NHERF and E3KARP, the binding affinity of NHERF for E3KARP was estimated by surface plasmon resonance spectroscopy (BIAcore) (Fig. 3A and Table 1). Sensorgrams of NHERF binding to E3KARP were used to calculate kinetic binding constants. Background sensorgrams were then subtracted from the experimental ones to yield representative specific binding constants. We found that NHERF indeed bound to E3KARP with an apparent K_D of 7 nM.

The fluorescence emission spectra of the purified NHERF and E3KARP revealed and the λ_{max} to be at 345 nm (Fig. 3B). The spectrum of the NHERF-E3KARP complex was a little lower than that of E3KARP alone. Simply combining the spectra of NHERF and E3KARP does not equal the spectrum of the NHERF-E3KARP complex. The fluorescence intensity was about 3,800 N for NHERF but only 700 N for E3KARP (Fig. 3B). At 24 °C, NHERF and E3KARP were mixed together in a 1:1 molar ratio at 5 μM each. A tight interaction is most likely accompanied by significant conformational changes in either one or both proteins and is likely facilitated at room temperature since the residues of aromatic groups are buried within the

Table 1. Kinetic parameters of binding of NHERF to E3KARP[a]

Concs of analyte (nM)	k_a ($M^{-1}s^{-1}$)	k_d (s^{-1})	K_D (M)
319	1.52×10^5	2.07×10^6	1.64×10^{-8}
159	3.57×10^5	2.49×10^{-3}	6.98×10^{-9}
80	6.97×10^5	2.69×10^{-3}	3.86×10^{-9}
20	2.07×10^6	3.13×10^{-3}	1.51×10^{-9}
K_D (nM)$_{avg}$			7.19

[a]The association rate constant (k_a) was determined from a plot of In[Abs (dR/dt)] *versus* time, where R is the intensity of the surface plasmon resonance signal at time t. The dissociation rate constant (k_d) was determined from a plot of In(R_0/R) *versus* time, where R_0 is the resonance signal intensity at time zero. The apparent K_D was calculated from the kinetic constants K_D (M) = k_d/k_a.

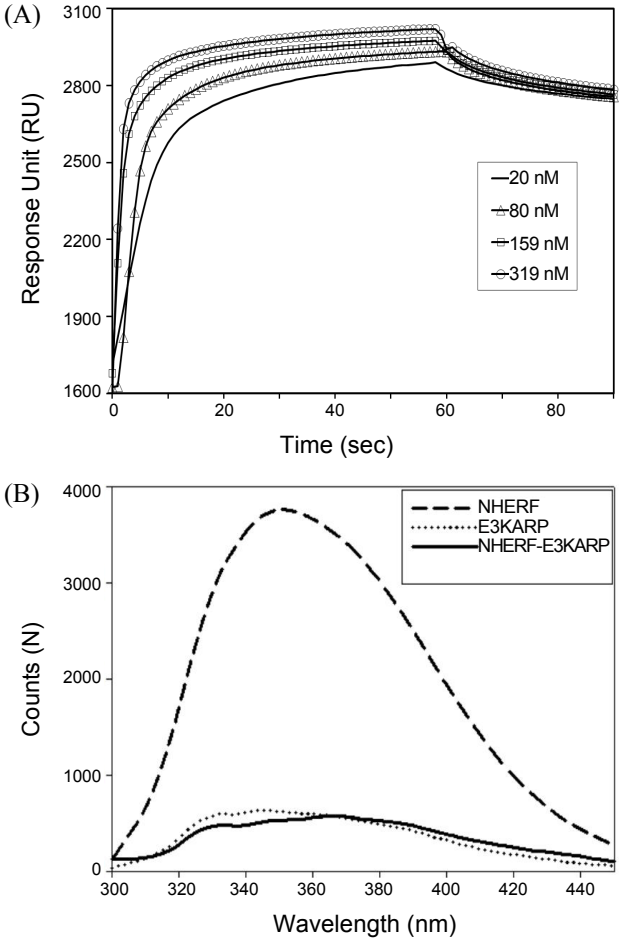

Figure 3. (A) BIAcore biosensor analysis of NHERF binding to E3KARP at 25 °C. The sensorgrams for 20, 80, 159 and 319 nM human E3KARP are shown. (B) Fluorescence analysis of NHERF binding to E3KARP. Fluorescence spectra of the NHERF-E3KARP complex and of each individual protein are shown.

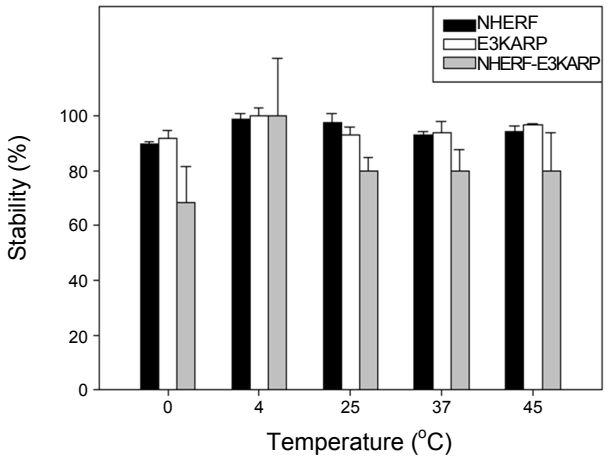

Figure 4. NHERF and E3KARP stabilities at various temperatures. The protein stability reactions were carried out for 10 min at various temperatures at a wavelength of 280 nm. The buffer for experiments contained 50 mM Tris-HCl [pH7.5], 200 mM NaCl, 1 mM DTT and 0.1 mM PMSF. At 4 °C, the optimum stabilities are shown.

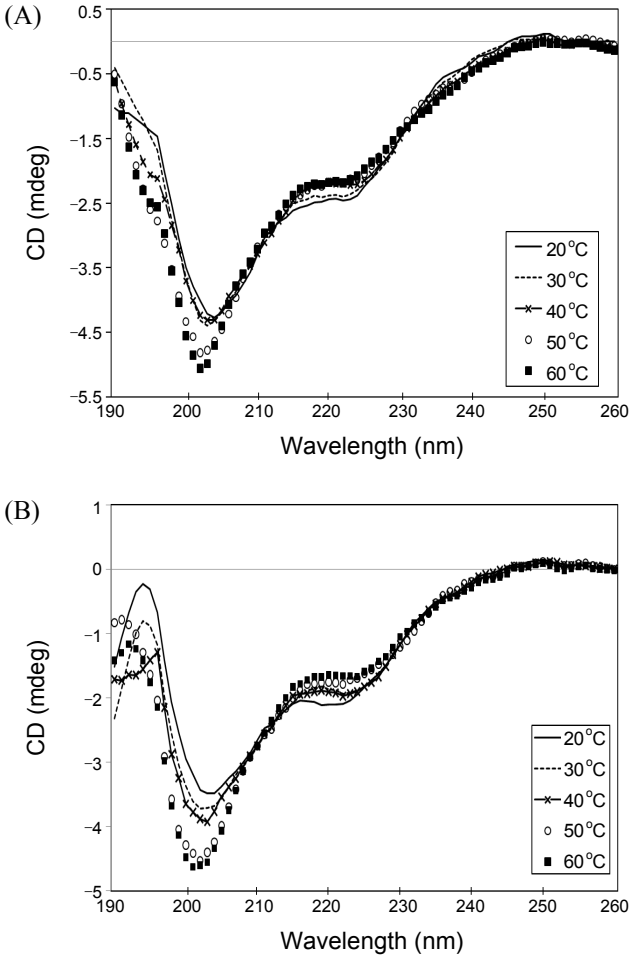

Figure 5. Far-UV CD spectra of NHERF and E3KARP. The CD spectrum was measured from 190 to 260 nm, and the CD signal was merged into CDNN. The experiment was carried out using a JASCO J-715 spectropolarimeter with a 0.1 cm cell at 0.2 nm intervals and 25 °C. These spectra were the result of 10 scans. A and B) CD spectra of the NHERF and E3KARP proteins at different temperatures (20 °C - 60 °C).

three-dimensional protein structure. Further, the less rigid, hydrophobic environment required for the conformational changes of NHERF and E3KARP can be initiated by a decrease in fluorescence intensity.

To examine the effects of temperature on protein stability, NHERF, E3KARP and the NHERF-E3KARP complex were incubated at various temperatures (0 - 45 °C) for 10 min (Fig. 4). The amount of soluble protein remaining after incubation was quantified using a BioPhotometer at 280 nm. NHERF, E3KARP and the NHERF-E3KARP complex all showed optimal stability at 4 °C. Interaction of NHERF with E3KARP stabilized the formation of other protein complexes as well as ligand interaction by the PDZ and EB domains in signaling pathways.

Thermal denaturation experiments for folded NHERF and E3KARP were carried out by CD spectroscopy. The CD spectra of the folded NHERF and E3KARP proteins at various temperatures from 20 to 60 °C are presented in Figure 5A and B, which shows two negative maxima at 204 and 220 nm. An interesting point is that the spectra show more α-helical characteristic bands at low temperatures. Heating caused progressive unfolding of the protein, loss of α-helix and appearance of

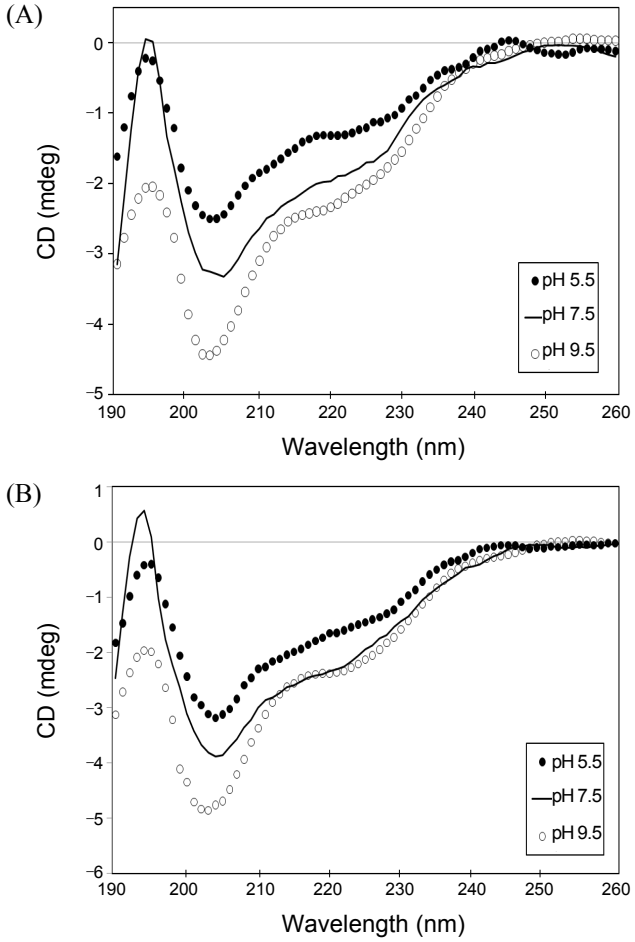

Figure 6. (A) and (B) Effects of pH on the CD spectra of NHERF and E3KARP. CD Spectra changes of NHERF and E3KARP at pH 5.5, 7.5 and 9.5 are shown. The detailed experimental methods are shown in Figure 5.

characteristic β-sheets. With a gradual increase in temperature, the occurrence of random coils and general characteristics of disordered or loosely-folded proteins was decreased. Both NHERF and E3KARP proteins showed relative stability upon temperature changes.

To observe the folding properties of NHERF and E3KARP, the proteins were observed under various pH conditions by CD spectroscopy (Fig. 6A and B). These results show that the CD curve at pH 9.5 was the deepest negative peak and the peak at pH 5.5 was the least negative one. NHERF and E3KARP at pH 7.5 were composed of a highly alpha-helical structure. The turnover of α-helix content in both proteins occurred at pH 7.5. Protein structures are, in general, strongly dependent on the solution conditions such as pH. As such, pH changes induce protonation-deprotonation of dissociable groups of proteins, including the carboxylic acid (aspartic acid and glutamic acid) and amine (lysine, arginine and histidine) side groups. Due to changes in charge density, the electrokinetic properties of the proteins also varied with pH. Therefore, an unfolded state corresponding to an extremely low pH will be observed if all of the ionizable side chains in NHERF and E3KARP become fully protonated or deprotonated. Na^+/H^+ exchangers display sensitivity to changes in intracellular pH and cell volume and are modulated by reagents primarily targeting serine/threonine and tyrosine kinases. Na^+/H^+ exchange exchanger isoform (NHE) 3 also plays an essential role in the maintenance of systemic pH homeostasis *via* Na^+ and HCO_3^- reabsorptive processes in renal proximal tubules.[22] The CD spectra of NHERF and E3KARP show that pH affected the conformational changes of the proteins to varying extents (Fig. 6A and B). These results are consistent the secondary structure of the protein predicted in Figure 1B. Exposing the protein to pH 5.5 and 9.5 significantly changed the conformations of the α-helices, β-sheets and random coils. The CD spectrum at pH 7.5, except for its negative peak depth, resembled that of the pH 5.5 and 9.5 spectra. These pH-dependent changes in the secondary structures of the proteins can be due to either local structural perturbation or an increased amount of unfolded protein in solution. The secondary structural elements and conformational properties of NHERF were almost similar to those of E3KARP. A conformational change by low or high pH was induced. The pH 9.5 form was more thermostable than the pH 5.5 form.

In the present study, we demonstrate *via* a series of biochemical and biophysical measurements that NHERF interacted strongly with E3KARP *in vitro*. Intriguingly, NHERF bound with high affinity to E3KARP. Further, the CD spectra of NHERF and E3KARP show that conformational changes of the proteins were dependent on pH and temperature conditions. Biochemical and biophysical studies suggest that the NHERF and E3KARP proteins perform overlapping functions as regulators of transmembrane receptors, transporters and other proteins localized at or near the plasma membrane wherever they coexist. Therefore, this study may provide important clues to the structural identification of signaling pathways involving NHERF and E3KARP.

Acknowledgments. This study was supported by the National R&D Program for Cancer Control, Ministry of Health & Welfare, Republic of Korea (0720110) to S.B.J.

References

1. Fanning, A. S.; Anderson, J. M. *J. Clin. Invest*. **1999**, *103*, 767-772.
2. Bezprozvanny, I.; Maximov, A. *Proc. Natl. Acad. Sci. USA* **2001**, *98*, 787-789.
3. Brenman, J. E.; Chao, D. S.; Gee, S. H.; McGee, A. W.; Craven, S. E.; Santillano, D. R.; Wu, Z.; Huang, F.; Xia, H.; Peters, M. F.; Froehner, S. C.; Bredt, D. S. *Cell* **1996**, *84*, 757-767.
4. Lim, S.; Naisbitt, S.; Yoon, J.; Hwang, J.; Suh, P.; Sheng, M.; Kim, E. *J. Biol. Chem*. **1999**, *274*, 29510-29518.
5. Daniels, D. L.; Cohen, A. R.; Anderson, J. M.; Brünger, A. T. *Nat. Struct. Biol.* **1998**, *5*, 317-325.
6. Tochio, H.; Zhang, Q.; Mandal, P.; Li, M.; Zhang, M. *Nat. Struct. Biol.* **1999**, *6*, 417-421.
7. Kozlov, G.; Gehring, K.; Ekiel, I. *Biochemistry* **2000**, *39*, 2572-2580.
8. Hillier, B. J.; Christopherson, K. S.; Prehoda, K. E.; Bredt, D. S.; Lim, W. A. *Science* **1999**, *284*, 812-815.
9. Karthikeyan, S.; Leung, T.; Birrane, G.; Webster, G.; Ladias, J. A. A. *J. Mol. Biol.* **2001**, *308*, 963-973.
10. Karthikeyan, S.; Leung, T.; Ladias, J. A. A. *J. Biol. Chem.* **2001**, *276*, 19683-19686.
11. Lamprecht, G.; Seidler, U. *Am. J. Physiol. Renal Physiol Gastro-*

intest Liver **2006**, *291*, G766-G777.
12. Weinman, E. J.; Steplock, D.; Shenolikar, S. *Kidney Int.* **2001**, *60*, 450-454.
13. Yun, C. H.; Lamprecht, G.; Forster, D. V.; Sidor, A. *J. Biol. Chem.* **1998**, *273*, 25856-25863.
14. Zizak, M.; Lamprecht, G.; Steplock, D.; Tariq, N.; Shenolikar, S.; Donowitz, M.; Yun C. H.; Weinman, E. J. *J. Biol. Chem.* **1999**, *274*, 24753-24758.
15. Short, D. B.; Trotter, R. W.; Reczek, D.; Kreda, S. M.; Bretscher, A.; Boucher, R. C.; Stutts, M. J.; Milgram, S. L. *J. Biol. Chem.* **1998**, *273*, 19797-19801.
16. Hall, R. A.; Premont, R. T.; Chow, C. W.; Blitzer, J. T.; Pitcher, J. A.; Claing, A.; Stoffel, R. H.; Barak, L. S.; Shenolikar, S.; Weinman, E. J.; Grinstein, S.; Lefkowitz, R. J. *Nature*. **1998**, *392*, 626-630.
17. Maudsley, S.; Zamah, A. M.; Rahman, N.; Blitzer, J. T.; Luttrell, L. M.; Lefkowitz, R. J.; Hall, R. A. *Mol. Cell. Biol*. **2000**, *20*, 8352-8363.
18. Guerra, L.; Fanelli, T.; Favia, M.; Riccardi, S. M.; Busco, G.; Cardone, R. A.; Carrabino, S.; Weinman, E. J.; Reshkin, S. J.; Conese, M.; Casavola, V. *J. Biol. Chem*. **2005**, *280*, 40925-40933.
19. Park, K. S.; Jeong, M. S.; Kim, J. H.; Jang, S. B. *Protein Expression & Purification* **2005**, *40*, 197-202.
20. Gerald, B. CD spectroscopy deconvolution, version 2.1 1997.
21. Takahashi, Y.; Morales, F. C.; Kreimann, E. L.; Georgescu, M. M. *EMBO J*. **2006**, *25*, 910-920.
22. Aronson, P. S.; Igarashi, P. *Curr. Topics Membr. Transport* **1986**, *26*, 57-75.